Available online at www.sciencedirect.com
ScienceDirect
Journal of Hazardous Materials 157 (2008) 170–178
Journal of Hazardous Materials
www.elsevier.com/locate/jhazmat

The effects of calcium hydroxide on hydrogen chloride emission characteristics during a simulated densified refuse-derived fuel combustion process

Kung-Yuh Chiang [a,*], Jer-Chyuan Jih [a], Kae-Long Lin [b]

[a] *Department of Environmental Engineering and Science, Feng-Chia University, Tai-Chung 407, Taiwan*
[b] *Department of Environmental Engineering, National I-Lan University, I-Lan, Taiwan*

Received 27 April 2007; received in revised form 26 November 2007; accepted 26 December 2007
Available online 5 January 2008

Abstract

This study investigated the effects of different calcium hydroxide ($Ca(OH)_2$) addition methods on the potential for hydrogen chloride (HCl) formation in a simulated densified refuse-derived fuel (RDF-5) with single metal combustion system. These experiments were conducted at 850 °C with the $Ca(OH)_2$ spiked in the RDF-5 production or injection in the flue gas treatment system. The results indicated that the potential for HCl formation was decreased significantly by $Ca(OH)_2$ spiked in the RDF-5 production or injection in the flue gas treatment system. However, the $Ca(OH)_2$ injection method in the flue gas for HCl emission reduction was better than other method. According to the relationship between the HCl emission and amount of $Ca(OH)_2$ injected or spiked, it is interesting to find that when the $Ca(OH)_2$ injected or spiked ranged from 0% to 5%, the potential for HCl formation in the single metal combustion system decreases significantly with increasing $Ca(OH)_2$ injected or spiked ratio. A corresponding increase in the amount of $CaCl_2$ partitioned to the fly ash was observed. However, with the ratio of $Ca(OH)_2$ higher than 5%, the amount of HCl formation showed that no further significant variation occurred with increasing $Ca(OH)_2$ spiked ratio.

Keywords: Refuse-derived fuel (RDF-5); Hydrogen chloride (HCl); Heavy metal

1. Introduction

Thermal treatment using incineration technology has been proven an attractive municipal solid waste (MSW) transformation method for many years due to the hygienic control, volume reduction and energy recovery advantages. In recent years, the focus has changed in response to increasing public and environmental concerns with pollutant emissions from MSW incinerators. Under these circumstances, MSW may be processed to obtain a fuel for direct utilization to generate electricity provided it has sufficient quality for employment instead of traditional fuels. Therefore, the advanced thermal treatment of refuse-derived fuel (RDF) has started to receive wide attention. In Taiwan, the establishment of a pilot plant for RDF production was sponsored by the Ministry of Economics in Eastern Taiwan (Hwa-Lian County) in 2003. The Taiwan Environmental Protection Administration (EPA) proposed a demonstration project for construction in which one materials recovery facility (MRF) to manufacture RDF was established [1]. The power generation of industrial process using RDF has attracted much attention. RDF is manufactured using industrial or agricultural waste, such as waste plastics, waste rubber, rejected sludge from paper processing, wood and saw dust, etc. The application potential for RDF will be an important strategy in Taiwan's waste management development.

RDF burning results in a higher average heating value for the waste stream destined for incineration, a lower possibility of toxic substance emissions due to complete combustion, and higher energy recovery potential, compared to MSW used as fuels. With higher heating value in the RDF product, better energy recovery efficiency could also be achieved from the engineering perspective [2]. Although RDF presents several advantages as an alternative fuel, however, in particular, RDF production without separation or incomplete separation of MSW components at the source, chlorines from PVC, food residues, and various other sources may significantly

* Corresponding author. Tel.: +886 4 24517250x5216; fax: +886 4 24517686.
E-mail address: kychiang@fcu.edu.tw (K.-Y. Chiang).

0304-3894/$ – see front matter © 2008 Elsevier B.V. All rights reserved.
doi:10.1016/j.jhazmat.2007.12.103

enhance the formation of metal chlorides in the RDF combustion.

Chlorine reacts with other elements to form toxic materials that react with hydrogen to form hydrogen chloride (HCl), or react with metals to form metal chlorides. The influence of HCl on the speciation of volatile metals, for instance, Pb, Sb, Cd, As, Zn and Ni would react to form chloride when a high HCl concentration exists in the exhaust gas [3].

The most of previous studies focused on the flue gas behavior and HCl emission characteristics during RDF combustion in a fluidized-bed incinerator [4–8]. However, little information has been developed about the HCl emission characteristics using RDF combustion in a fixed-bed incinerator. There will be different combustion characteristics between fluidized-bed and fixed-bed incinerator. The high chlorine content in MSW, which is especially critical in Taiwan as the local MSW is characterized by high plastic content (average of 20%) and food residue content (average of 26%) [1], which respectively contributes most of the organic and inorganic chlorides for HCl formation. Therefore, to minimize the risks of HCl emissions, it is essential to obtain a better understanding of the toxic pollutant emission characteristics during the RDF combustion process. The objective of this research was to investigate the effects of calcium hydroxide ($Ca(OH)_2$) on the potential for HCl formation during a simulated densified RDF-5 with single metal (Cd, Pb, Cu, Cr, and Zn) combustion system. The results of this study may be of interest to operators and administrators attempting to minimize HCl emissions and optimize the $Ca(OH)_2$ dosage, and to researchers interested in the engineering aspects of RDF-5 combustion.

2. Materials and methods

2.1. Commercial RDF-5 and preparation of simulated RDF-5

In this study, five kinds of RDF-5 samples were collected from pilot scale materials recovery facilities (MRFs) and made from combustibles in the source-separated MSW (RDF-5-a), plastics in the MSW (P-RDF-5-a), plastics and rubber scraps in the industrial manufacturing process (P-RDF-5-b and R-RDF-5), paper rejected sludge from a paper mill plant (PR-RDF-5), and wood waste (W-RDF-5), respectively.

The simulated RDF-5 samples selected for use in the simulated MSW were paper, textiles, wood, food waste and plastics, which are materials of waste samples made up to simulate RDF-5 that might be combusted in a laboratory incinerator. Dried waste samples were blended to produce homogenous mixes with $Ca(OH)_2$ additions of 0, 5, 10, 20, and 25% (by weight) of a dry basis. Uniaxially pressed 'densified' RDF-5 samples were prepared by adding 50 wt.% water to the dry sample and pressing at 60 kgf/cm^2 (800 psi) for 30 min. This formed cylindrical RDF-5 specimens approximately 50 mm in height and 20 mm in diameter. Samples free of $Ca(OH)_2$ RDF-5 were also prepared using the same procedures. This was done to compare the efficiency of $Ca(OH)_2$ injection in the flue gas for HCl removal during the RDF-5 combustion process. To simulate the background metal concentrations in RDF-5, simulated and representative RDF-5 trace metal sample concentrations were adjusted and spiked with powdered forms of Pb, Cd, Cr, Cu, and Zn acetate compounds, respectively.

2.2. Experimental facility and operation procedure

A schematic diagram of the experimental device is shown in Fig. 1. The apparatus used in this study was composed of an electric-heated tube furnace and a sampling train of impingers. The heart of the furnace was a quartz tube burner, 85 cm long and 5.5 cm in inner diameter, housed in a glassfiber-lined insulated steel shell. A quartz boat moved with a quartz rod was prepared, to feed the RDF-5 into the combustion chamber. The combustion temperature at the center inside the burner tube was monitored using a thermocouple and controlled by a programmed temperature controller. Lime solution (5% by weight) was pumped into the flue gas to react with the acidic gas.

Downstream from the combustion chamber a quartz-fiber filter was set up. To prevent the flue gases from condensing while flowing through the filter, the filter together with its holder

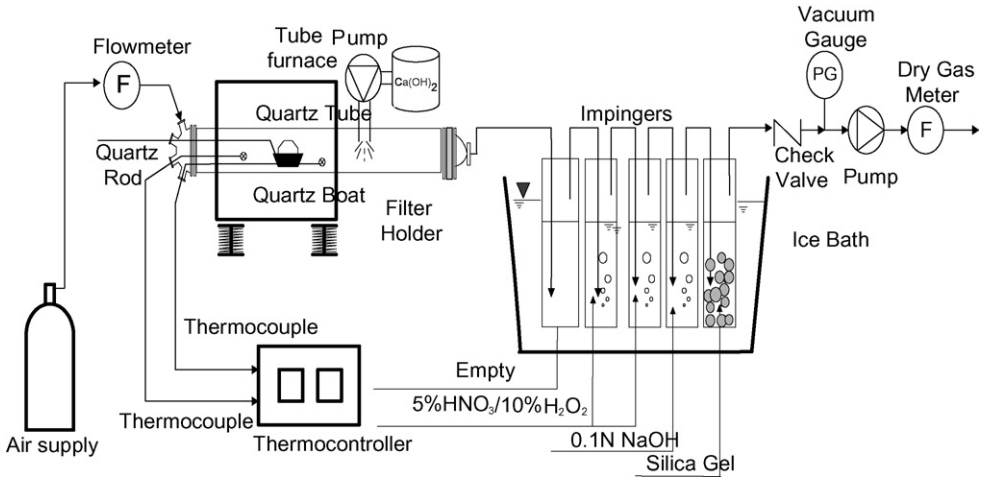

Fig. 1. Schematic diagram of RDF-5 combustion and HCl sampling.

Table 1
The principal properties and the metal contents of the RDF-5

	RDF-5-a	P-RDF-5-a	W-RDF-5-a	W-RDF-5-b	W-RDF-5-c	PR-RDF-5	P-RDF-5-b	R-RDF-5	Simulated RDF-5
HHV (Kcal/kg)	4256.3 ± 309.3	9457.6 ± 667.7	3980.0 ± 189.5	3886.8 ± 110.3	3744.4 ± 141.1	4673.4 ± 83.5	5061.1 ± 781.8	4807.5 ± 528.9	2634.8
Proximate analysis (wt.%)									
Moisture	8.05 ± 2.75	0.68 ± 0.12	13.10 ± 0.08	6.94 ± 0.03	10.02 ± 0.99	6.97 ± 0.43	10.98 ± 11.21	2.44 ± 0.48	47.6
Combustible	75.68	96.01	78.22	79.29	80.24	85.6	74.89	69.20	47.2
Ash	16.27 ± 3.24	3.31 ± 1.12	8.68 ± 1.00	13.77 ± 0.79	9.74 ± 1.14	7.43 ± 0.71	14.13 ± 11.52	28.36 ± 0.16	5.2
Ultimate analysis (wt.%)									
C	33.3 ± 4.01	74.92 ± 2.37	35.54 ± 0.18	33.48 ± 1.83	48.25 ± 0.29	42.24 ± 2.58	40.71 ± 10.47	33.71 ± 4.00	36.94
H	5.16 ± 1.07	16.33 ± 2.72	5.21 ± 0.14	4.98 ± 0.44	6.62 ± 0.37	5.59 ± 0.26	6.42 ± 1.31	3.83 ± 0.31	3.15
O	35.68	3.00	34.88	36.73	16.71	37.14	25.04	27.10	2.08
N	0.61 ± 0.43	0.03 ± 0.01	0.96 ± 0.07	1.99 ± 0.37	2.11 ± 0.29	0.01 ± 0.00	0.59 ± 0.54	0.56 ± 0.49	3.19
S	0.50 ± 0.30	0.26 ± 0.10	0.56 ± 0.04	0.73 ± 0.06	4.88 ± 0.29	0.32 ± 0.00	0.76 ± 0.23	0.93 ± 0.07	0.34
Cl	0.43 ± 0.30	1.47 ± 1.11	1.08 ± 0.1	0.35 ± 0.06	1.67 ± 0.29	0.30 ± 0.03	1.37 ± 2.41	3.07 ± 3.91	1.50
Metal analysis (mg/kg)									
Zn	499.25 ± 438.50	N.A.	N.A.	N.A.	12.0 ± 2.0	N.A.	N.A.	N.A.	1000
Cu	83.33 ± 146.04	N.A.	N.A.	N.A.	6.4 ± 0.6	N.A.	N.A.	N.A.	1000
Pb	365.62 ± 383.47	N.A.	N.A.	N.A.	30.0 ± 7.6	N.A.	N.A.	N.A.	1000
Cd	1.72 ± 2.78	N.A.	N.A.	N.A.	1.4 ± 0.6	N.A.	N.A.	N.A.	1000
Cr	56.79 ± 35.88	N.A.	N.A.	N.A.	<0.6	N.A.	N.A.	N.A.	1000

RDF-5-a: refuse-derived fuel (sample no. 15); PDF-5-a: household plastic-derived fuel (sample no. 5); PDF-5-b: industrial plastic-derived fuel (sample no. 5); WDF-5-a,b,c: wood-derived fuel (sample no. 5); PrDF-5: paper rejects-derived fuel (sample no. 5); RrDF-5: rubber-derived fuel (sample no. 3); simulated RDF-5: samples were made from a blend of paper, textile, wood, food waste, and plastics. N.A.: not available.

remained at a temperature above 200 °C. The filter was 99.97% effective in the removal of 0.3-μm particles during the test conditions. The sampling train consisted of five impingers in a series followed by the filter. The flue gas emission sample was drawn through the sampling train in which a quartz filter captured the particulate matter and acidic impinger solutions captured the metals or acidic gas in the flue gases.

Acidic absorbing solutions for the multiple metals were used in two of the five impingers in the sampling train. An impinger solution composed of 5% nitric acid and 10% hydrogen peroxide was used in the second and third impingers followed by the empty first impinger to capture the majority of these metal emissions. A 0.1N solution of sodium hydroxide (NaOH) was used in the forth impinger which absorbed the HCl. Silica gel filled in the fifth impinger to remove the water content in the flue gas.

The experiments were conducted at 850 °C. The RDF-5 was loaded in the quartz boat and pushed forward into the central part of the combustion chamber when the given temperature was reached. Combustion air was supplied by an air compressor at a flow rate of about 1.4 L/min at room temperature, under one unit atmospheric pressure, which corresponded to 50% excess air. The combustion time was pre-determined for each batch as the time when ignition loss in the RDF-5 residues became equal to or less than 5% (w/w). The retention time of the flue gas was estimated about 1.0 s. At the end of each batch combustion, the residues in the quartz boat were collected as bottom ash; particulates on the filter were gathered as air pollution control residues (APC residues). Combustion gas samples were taken from the impingers.

2.3. Analysis methods

The moisture content of RDF-5 and simulated RDF-5 samples were determined by heating for 24 h at 105 °C. The combustible and ash fraction of the samples were determined in triplicate using American Public Health Association (APHA) Standard Methods [9]. The ultimate analysis of the combustible in the RDF-5 was also analyzed in triplicate using an elemental analyzer (PerkinElemer, PE 2400 Series). The energy content of RDF-5 was determined using a laboratory bomb calorimeter (Parr 1341 calorimeter).

All ash and aqueous samples were collected as previously described and analyzed using flame atomic adsorption spectroscopy (FAAS) to determine the partitioning characteristics of Pb, Cd, Zn, Cr, Cu, and Ca. Metal concentrations measured in the bottom ash, the APC residues and the flue gases were used to determine the metal contents and calculate the amount of heavy metal partitioned into each fraction. Based on the determined metal contents, the normalized metal partitions were calculated as the ratio of the mass of each target metal in the bottom ash, fly ash, and flue gas, respectively, to the total mass of the metal in the above discharges. The collected bottom ash and APC residues were washed with ion-free water to extract the chlorine. The extracted ashes and aqueous samples were analyzed using ion chromatography (IC, Dionex, DI-100). The X-ray powder diffraction (XRD, MAC Science, MXP3) was widely applied to speciate any crystalline phase present in the ashes and to identify the metal species formation.

3. Results

3.1. Properties of RDF-5

Table 1 shows the moisture content, combustible fraction, percentage ash, heating value, ultimate analysis, and metals content (mg/kg) data for the different RDF-5 samples and simulated RDF-5. The simulated RDF-5 manufactured in the laboratory is shown in Table 1 for comparison. The overall average moisture content in the different RDF-5 samples was around 0.68–13.10%. This is due to the RDF-5 production using the drying process before the application. The combustible fractions of the RDF-5 were above 70%, especially for RDF-5 manufactured from plastics in the MSW (P-RDF-5-a) was highly combustible fraction (96.01%). Consequently, the P-RDF-5-a has highest heating value (HHV) than other tested RDF-5 samples. The average heating value was found to be around 3744.4 kcal/kg to 9457.6 kcal/kg. This means that the heating value of RDF-5 is similar to that of coal. However, RDF-5 is manufactured from different waste sources and has comparatively variable characteristics. The chlorine content of RDF-5 was actually high (from $1.08 \pm 0.1\%$ to $3.07 \pm 3.91\%$). Therefore, the HCl emission will be taken into consideration during the RDF-5 combustion process.

The total metal concentrations in RDF-5 manufactured from MSW were higher than other sources of RDF-5. The Zn and Pb concentrations in RDF-5 manufactured from MSW (RDF-5-a) were typically 499.25 ± 438.50 mg/kg for Zn and 365.62 ± 383.47 mg/kg for Pb. Other concentrations of tested metals were 83.33 ± 146.04 mg/kg for Cu, 59.79 ± 35.88 mg/kg for Cr, 1.72 ± 2.78 mg/kg for Cd, respectively. The background concentrations of metals in simulated RDF-5 materials were much lower than the actual RDF-5 measurement. Therefore, preparation of simulated RDF-5 samples for trace metal con-

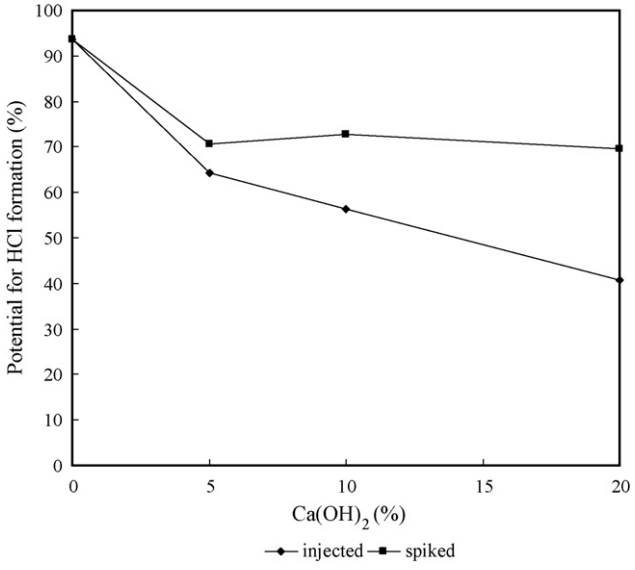

Fig. 2. HCl formation potential in combustion of RDF-5 with Cd spiked.

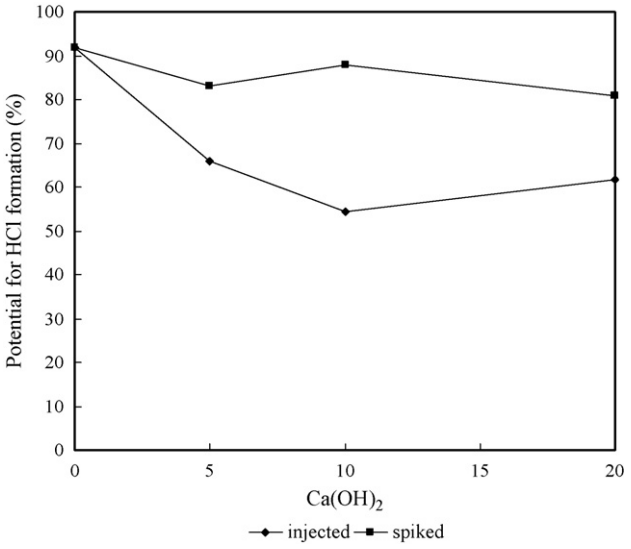

Fig. 3. HCl formation potential in combustion of RDF-5 with Zn spiked.

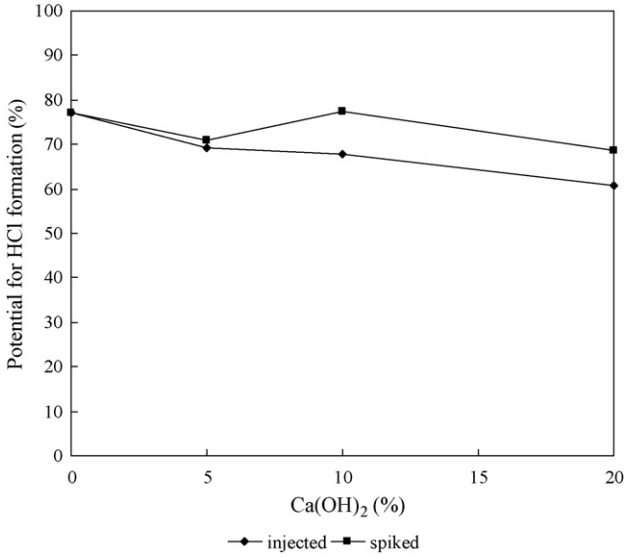

Fig. 4. HCl formation potential in combustion of RDF-5 with Cu spiked.

centration was adjusted by spiking metal medium to represent the behavior of waste-based metals in the incineration. To simplify the effect of the metals concentration on HCl formation during the RDF-5 combustion process the total metal concentrations of Zn, Pb, Cu, Cr, and Cd in simulated RDF-5 were 1000 mg/kg, respectively.

3.2. Effect of $Ca(OH)_2$ on HCl formation potential

In the RDF-5 combustion process, HCl formation is a complex process, involving the availability of chlorine, a hydrogen source, and the competitive affinity of the tested metals. In general, the reactive affinity between hydrogen and chlorine is stronger than that between the heavy metals and chlorine [10]. In this research, the HCl formation potential (HFP) is defined as follows [11,12]:

$$\mathrm{HFP\,(HCl\ \ formation\ \ potential,\ mg\ \ HCl/mg\ \ Cl)} = \frac{\mathrm{mass\ \ of\ \ chlorine\ \ (HCl)\ \ in\ \ the\ \ flue\ \ gas}}{\mathrm{input\ \ chlorine\ \ in\ \ the\ \ RDF-5\ \ sample}}$$

As shown in Fig. 2, the formation ratio of HCl in a single Cd combustion system showed a decrease when the $Ca(OH)_2$ content increased. For the injection system, the results indicate that the percentage of HCl formation potential was 93.71% without injecting any $Ca(OH)_2$. However, when the $Ca(OH)_2$ injection ratio was raised to 20%, the HCl formation potential decreased to 40.68%. In the spiked system, the results show that the percentage of HCl formation potential decreased to 70.76% with a 5% $Ca(OH)_2$ ratio. However, when the $Ca(OH)_2$ ratio was raised to 20%, the HCl formation potential decreased insignificantly. This was especially noteworthy in that the chlorine distribution in the APC residues increased with the decrease in chlorine distribution in the flue gas. This showed that $Ca(OH)_2$ supplied Ca^{2+} to react with Cl^- in the RDF-5 combustion system to form $CaCl_2$ in the APC residues according to the following reactions [13]:

$$\mathrm{Ca\,(OH)_2 \rightarrow\ CaO\ +\ H_2O}$$

$$\mathrm{CaO\ +\ 2HCl\ \rightarrow\ CaCl_2 + H_2O}$$

Fig. 3 shows the HCl formation potential effect for injected or spiked $Ca(OH)_2$ in single metal Zn combustion system. The results indicated that the HCl formation potential decreased rapidly from 91.48% to 54.34% when the $Ca(OH)_2$ injection ratio was increased from 0% to 10%, whereas the HCl formation potential slightly increased as 20% $Ca(OH)_2$ injection ratio. The similar phenomena occurred in spiked system, HCl formation potential was seen to decrease rapidly at 5% $Ca(OH)_2$ spiked ratio. In case of the single Cu combustion system, as indicated in Fig. 4, 20% $Ca(OH)_2$ tested ratio was effective in reducing the HCl formation potential for both injected and spiked $Ca(OH)_2$ systems. The HCl formation potential for injection

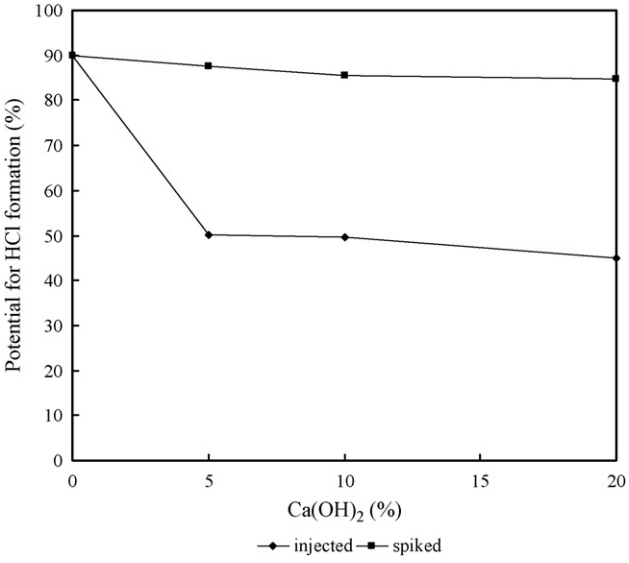

Fig. 5. HCl formation potential in combustion of RDF-5 with Cr spiked.

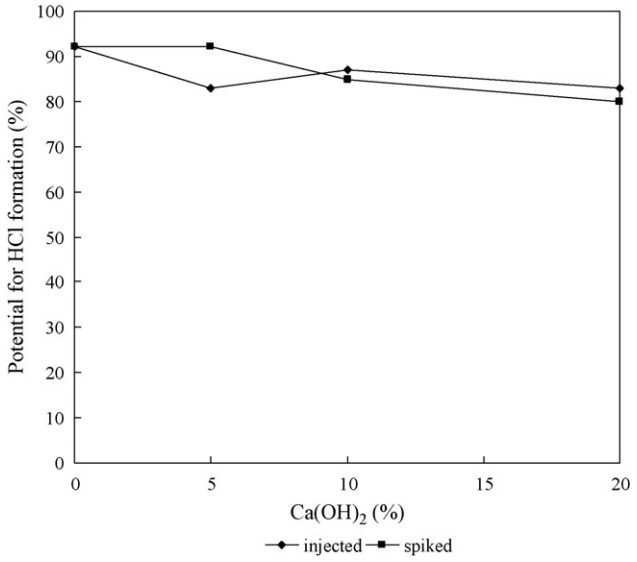

Fig. 6. HCl formation potential in combustion of RDF-5 with Pb spiked.

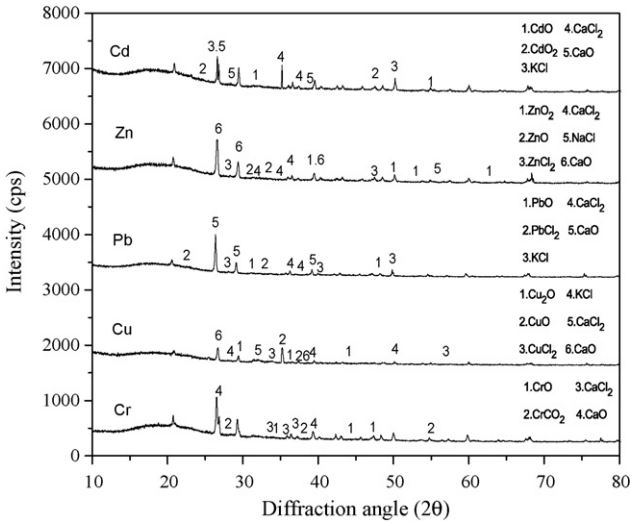

Fig. 7. X-ray diffraction pattern of the APC residues.

system reveals a decreasing tendency when the $Ca(OH)_2$ ratio ranges from 0% to 20%. Herein, an optimization of 60.74% formation potential ratio occurs at 20% injected $Ca(OH)_2$ tested condition. For the spiked system, the HCl formation potential was also seen to decrease from 77.08% to 70.83% with 5% $Ca(OH)_2$ spiked ratio. However, there is no significant effect of continuously increased $Ca(OH)_2$ spiked ratio to 20% on the reduction of HCl formation potential.

The potential for HCl emission in single metal Cr combustion system is shown in Fig. 5. The HCl removal efficiency was not obvious with an increase in the $Ca(OH)_2$ quantity in the spiked system. In the injection system, the HCl formation potential rapidly decreased from 89.87% to 44.98% with an increasing $Ca(OH)_2$ injection ratio. As the $Ca(OH)_2$ injection ratio was higher than 5%, the HCl formation potential was nearly constant. Fig. 6 also indicates that the HCl formation potential in single Pb combustion system decreases with an increasing $Ca(OH)_2$ injection or spiked ratio. As the $Ca(OH)_2$ injection ratio was 5%, the HCl formation potential decreased slightly from 92.11% to 82.89%. In the spiked system, the results show that the HCl formation potential did not change with 5% $Ca(OH)_2$ ratio. However, as the $Ca(OH)_2$ ratio increased to 20%, the HCl formation potential decreased from 92.11% to 80.00%.

3.3. Calcium partitioning in the APC residues

In this study, to further understand the effect of spiked or injected $Ca(OH)_2$ in providing Ca^{2+} to react with Cl^- to form $CaCl_2$ in APC residues, the quantity of Ca^{2+} in the APC residues was analyzed after each batch run. According to the results of Ca^{2+} content in the APC residues, the formation of $CaCl_2$ or CaO and their compounds deposited in the APC residues during RDF-5 combustion process could be supported. In this research, the partitioning of Ca^{2+} in the APC residues can be calculated as follows:

$$Ca^{2+}\ \text{partitioning percentage in APC residues} = \frac{Ca^{2+}\ \text{amount in APC residues (mg)}}{\text{total injected or spiked quantity of } Ca^{2+}\ \text{in the test (mg)}}$$

Table 2
The partitioning of Ca^{2+} in the fly ash

Single metal combustion system	$Ca(OH)_2$ spiked test			$Ca(OH)_2$ injection test (unit in %)		
	5%	10%	20%	5%	10%	20%
Cd	57.78	57.60	65.93	85.93	84.00	80.83
Zn	46.67	52.80	51.11	67.41	73.60	69.91
Pb	60.00	57.00	63.15	98.15	94.00	86.57
Cu	72.59	59.60	64.85	85.93	83.20	78.98
Cr	65.19	61.00	63.15	80.74	84.40	77.69

Table 2 indicates the partitioning of Ca^{2+} in APC residues in single metal combustion with a spike or injection $Ca(OH)_2$ system. In the spiked system case, the partitioning of Ca^{2+} ranged

Table 3
Gibb's free energy of the tested metals compounds as function of 800 °C and 900 °C

	Cd		Zn		Pb		Cu		Cr	
	$CdCl_2$	CdO	$ZnCl_2$	ZnO	$PbCl_2$	PbO	$CuCl_2$	CuO	$CrCl_3$	Cr_2O_3
800 °C	−706.33	−510.96	−767.02	−595.81	−411.48	−583.61	−608.55	−319.73	−1010.73	−1707.45
900 °C	−837.25	−608.57	−904.06	−692.33	−425.09	−623.62	−768.09	−401.81	−1186.89	−1935.60

$\Delta G_T^\circ = \Delta H_{298}^\circ + \int_{298}^{T} \Delta C_p dT - T\left(\Delta S_{298}^\circ - \int_{298}^{T} (\Delta C_p/T)\, dT\right)$, ΔH_{298}°: enthalpy at 298 K; ΔS_{298}°: entropy at 298 K; ΔC_p: constant-pressure specific heat.

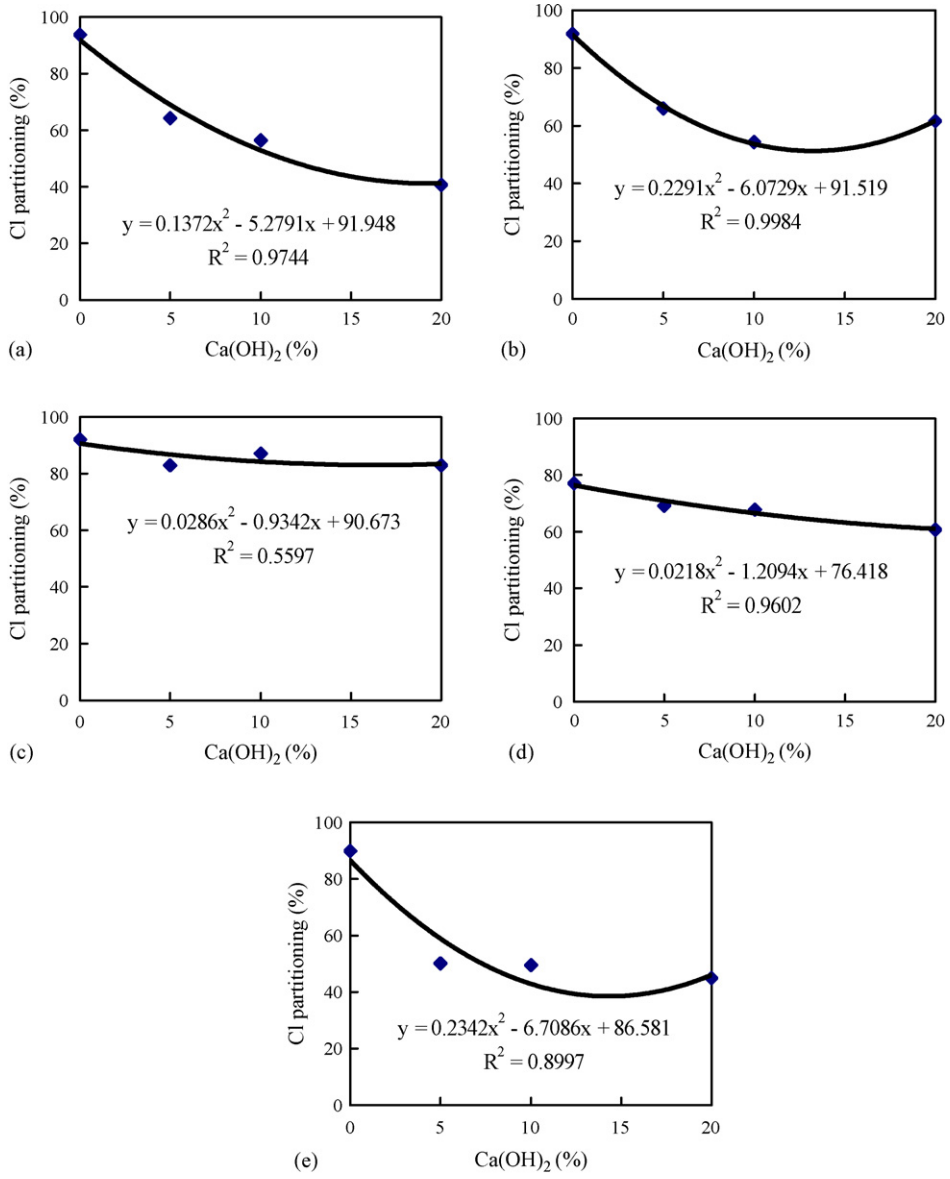

Fig. 8. Relationship between HCl partitioning in flue gas and $Ca(OH)_2$ injection amount. (a) Single Cd combustion system; (b) single Zn combustion system; (c) single Pb combustion system; (d) single Cu combustion system and (e) single Cr combustion system.

from 46.67% to 72.59% in the tested single metal combustion system. Meanwhile, in the injection system, the partitioning of Ca^{2+} was between 67.41% and 98.15% in the APC residues. This was greater than that from the spiked system. According to these results, whether in the injected or spiked system, the Ca^{2+} content was presented mainly in the APC residues. That is, the potential for reacting to form $CaCl_2$ was high and decreased the formation potential of HCl.

Table 4
Effects of $Ca(OH)_2$ on the HCl emission reduction rate

Metal	$Ca(OH)_2$ spiked				$Ca(OH)_2$ injected			
	0–5%	5–10%	10–20%	0–20%	0–5%	5–10%	10–20%	0–20%
Cd	−4.590	+0.408	−0.310	−1.201	−5.866	−1.574	−1.573	−2.652
Zn	−1.758	−0.010	−0.223	−0.514	−5.164	−2.336	+0.725	−1.513
Pb	+0.004	−1.450	−0.488	−0.606	−1.844	+0.834	−0.466	−0.459
Cu	−1.250	−0.166	−0.148	−0.428	−1.586	−0.264	−0.709	−0.817
Cr	−0.468	−0.416	−0.070	−0.256	−7.950	−0.126	−0.451	−2.245

−: decrement in HCl emission; +: increment in HCl emission; unit: %; data were defined as follows: ΔHCl content in flue gas (%)/Δ amount of $Ca(OH)_2$ spiked or injected.

3.4. Crystalline speciation analysis of APC residues

Fig. 7 shows the X-ray diffraction pattern of the APC residues. XRD results comparison for the RDF-5 with various metals spiked at a combustion temperature of 850 °C with 5% $Ca(OH)_2$ injection ratio indicated that similar species were identified. The major species present were CaO, $CaCl_2$, NaCl, and KCl. In addition, other tested metals oxide or chloride was presented in the APC residues and was in relation to the tested metals spiked. As previous results indicate, whether in the injected or spiked system, the $Ca(OH)_2$ will dehydrate and react with any type of chloride to form $CaCl_2$, simultaneously decreasing the formation potential of HCl. Meanwhile, due to incomplete reaction, CaO was also presented in the APC residues. The identification of NaCl or KCl in the APC residues throughout the tested $Ca(OH)_2$ ratio suggested that alkaline metals have a greater affinity to chlorine than do the other targeted heavy metals.

4. Discussion

To further discuss the relationship between the hydrogen chloride emission and optimum amounts of $Ca(OH)_2$ injected or spiked, the regression analysis method was used in this study. The HCl partition reduction curves in Figs. 8 and 9 exhibit two things: (1) the intercept indicates the HCl partition in the flue gas without any spiked or injected $Ca(OH)_2$ addition; and (2) the slope implies the reduction rate. The intercepts shown in Figs. 8 and 9 indicate that the partitioning of HCl in the flue gas without any $Ca(OH)_2$ addition ranges from 75% to 93%. In case of the single Cu combustion system, the partitioning of HCl in the flue gas was nearly 77.08%. This is due to the strong affinity of metal Cu to chlorine. Similarly, in case of the single Cr, Zn, Pb, Cu combustion system, the partitioning of HCl in the flue gas were 89.87%, 91.84%, 92.11%, and 93.71%, respectively. The results imply the affinity of metals to chlorine found to be Cu > Cr > Zn/Pb/Cd. This also suggests that metals with a

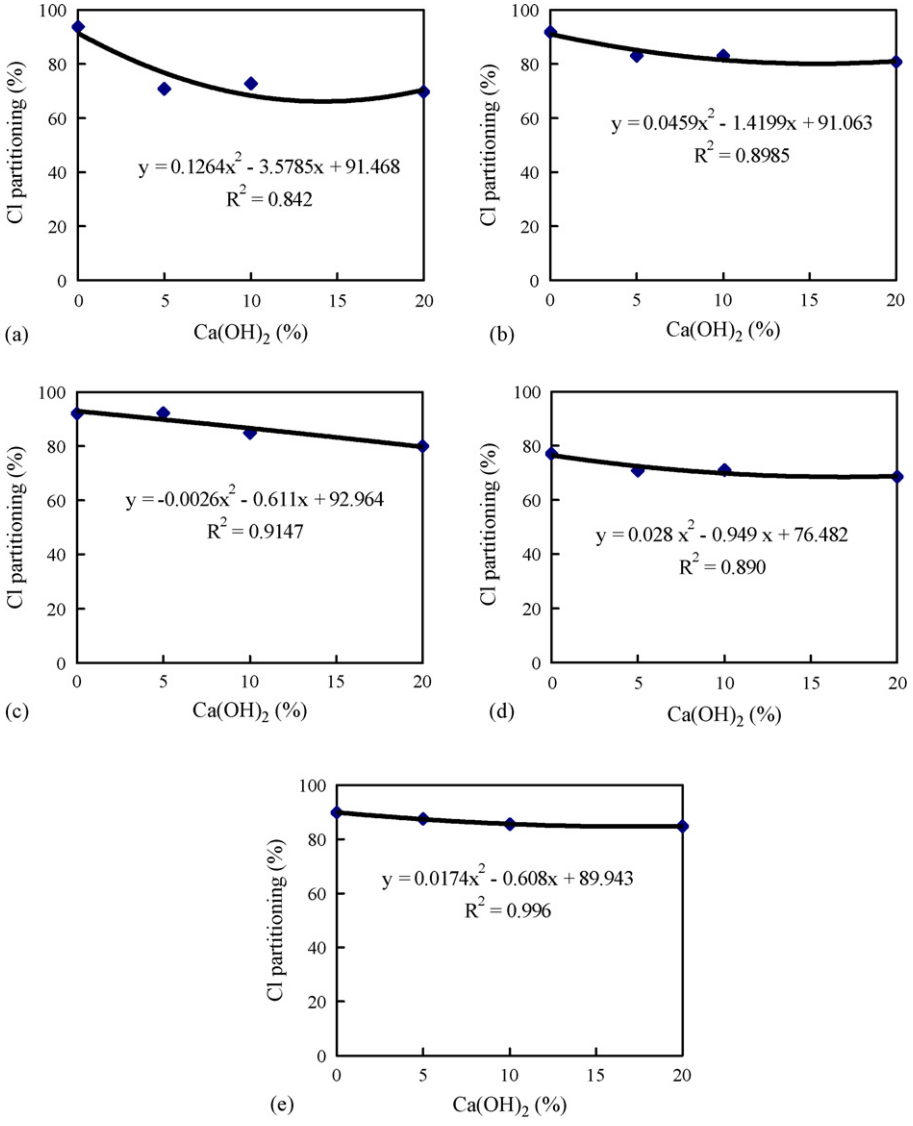

Fig. 9. Relationship between HCl partitioning in flue gas and amount of $Ca(OH)_2$ spiked. (a) Single Cd combustion system; (b) single Zn combustion system; (c) single Pb combustion system; (d) single Cu combustion system and (e) single Cr combustion system.

refractory volatility, such as Cr and Cu, have a stronger affinity to form metal chloride than the other tested metals with higher volatility (Zn, Pb, and Cd).

Accordingly, the theoretical thermodynamic (free energy) analysis results also showed that the formation potential of tested metals chloride was higher than other tested metals speciation (as shown in Table 3). Therefore, the presence of metals in RDF combustion system could reduce the HCl emission in the flue gas, but also could promote the potential for the metal chloride emission in the flue gas. The chloride effects on the metals partitioning during RDF combustion process are preferable and will be taken into consideration in further study.

Figs. 8 and 9 also show that the hydrogen chloride content in the flue gas had a negative correlation with the increase in the spiked or injected amount of $Ca(OH)_2$ during a single metal Cd, Zn, Pb, Cu, and Cr combustion system. That is, the hydrogen chloride partition in the flue gas decreases with increasing $Ca(OH)_2$ spiked content in the RDF or $Ca(OH)_2$ injected amount in the flue gas. In the case of injected $Ca(OH)_2$, the HCl formation potential reveals a decreasing tendency with increasing $Ca(OH)_2$ ratio, especially for single Cd combustion system. According to the regression analysis results, the correlation coefficient shows a great relationship between the $Ca(OH)_2$ ratio and HCl formation potential in the flue gas. The HCl removal efficiencies of single Zn and Cr combustion system with semi-dry ($Ca(OH)_2$) injection show the better efficiencies than spiked $Ca(OH)_2$ in the RDF-5 production. In the cases with 20% $Ca(OH)_2$ addition ratio and single Cd combustion system with $Ca(OH)_2$ injection or spiked, the maximum HCl removal efficiencies were 74.12% and 78.04%, respectively.

To facilitate interpretation, the slopes in Figs. 8 and 9 are summarized and given in Table 4. Table 4 shows that these slope values and the effects of the amount of $Ca(OH)_2$ on the reduction of HCl partitioned to the flue gas. The HCl emission reduction rate is formally defined as $\Delta\%$ HCl/$\Delta\%$ $Ca(OH)_2$, reflecting the variation in amount of HCl emission ($\Delta\%$ HCl) to the amount of $Ca(OH)_2$ injected or spiked ($\Delta\%$ $Ca(OH)_2$). In the case of spiked or injected $Ca(OH)_2$ test, the HCl emission reduction rate was dropped significantly at 5% $Ca(OH)_2$ spiked or injected amount. In addition, in case of $Ca(OH)_2$ spiked or injected amount above 10%, the increase in $Ca(OH)_2$ spiked or injected amount seems to have had no significant effect on the HCl reduction amount in the flue gas. In most cases the results shown in Table 4 are well correlated and demonstrate that the optimum ratio of spiked or injected $Ca(OH)_2$ on the reduction of HCl emission should be 5% $Ca(OH)_2$ addition.

5. Conclusions

(1) The metal species in the APC residues identified by X-ray diffraction (XRD) were tested metal oxide, calcium chloride ($CaCl_2$) and calcium oxide (CaO) in the single metal combustion system. That is, in the RDF-5 combustion process, injected or spiked $Ca(OH)_2$ will react with HCl and form $CaCl_2$ in the APC residues. Consequently, injected or spiked $Ca(OH)_2$ will promote decreasing the potential of HCl emission from the flue gas during the RDF-5 combustion process.

(2) The presence of metals in RDF combustion system could reduce the HCl emission in the flue gas, but also could promote the potential for the metal chloride emission in the flue gas. In this study, the reactive affinity of tested metals to chlorine was found to be Cu > Cr > Zn/Pb/Cd.

(3) According to the relationship between the HCl emission reduction rate and the amount of $Ca(OH)_2$ injected or spiked, the HCl emission reduction rate was decreased significantly at 5% $Ca(OH)_2$ spiked or injected amount. Meanwhile, in case of $Ca(OH)_2$ spiked or injected amount above 10%, the HCl emission reduction rate was decreased slowly with an increase in $Ca(OH)_2$ spiked or injected amount. This means that the optimum ratio of spiked or injected $Ca(OH)_2$ on the reduction of HCl emission will be 5% $Ca(OH)_2$ addition.

Acknowledgement

The authors would like to thank the Industrial Technology and Research Institute (ITRI), Hsin-Chu, Taiwan, ROC for financially supporting this work.

References

[1] Environmental Protection of Administration Executive Yuan, Taiwan, Republic of China, http://www.epa.gov.tw/.
[2] G. Piao, S. Aono, M. Kondoh, R. Yamazaki, S. Mori, Combustion test of refuse derived fuel in a fluidized bed, Waste Manage. 20 (2000) 443–447.
[3] B. Courtemanche, Y. Levendis, Control of the HCl emission from the combustion of PVC by in-furnace injection of calcium magnesium based sorbent, Environ. Eng. Sci. 15 (1998) 123–135.
[4] G.Q. Liu, Y. Itaya, R. Yamazaki, S. Mori, M. Yamahuchi, M. Kondoh, Fundamental study of the behavior of chlorine during the combustion of single RDF, Waste Manage. 21 (2001) 427–433.
[5] N. Kobyashi, Y. Itaya, G. Piao, S. Mori, M. Kondo, M. Hamai, M. Yamaguchi, The behavior of flue gas from RDF combustion in a fluidized bed, Powder Technol. 51 (2005) 87–95.
[6] J. Partanen, P. Backman, R. Backman, M. Hupa, Absorption of HCl by limestone in hot flue gases. Part I. The effects of temperature, gas atmosphere and absorbent quality, Fuel 84 (2005) 1664–1673.
[7] J. Partanen, P. Backman, R. Backman, M. Hupa, Absorption of HCl by limestone in hot flue gases. Part II. Importance of calcium hydroxychloride, Fuel 84 (2005) 1674–1684.
[8] J. Partanen, P. Backman, R. Backman, M. Hupa, Absorption of HCl by limestone in hot flue gases. Part III. Simultaneous absorption with SO_2, Fuel 84 (2005) 1685–1694.
[9] American Public Health Association (APHA), Standard Methods for the Examination of Water and Wastewater, 20th edition, American Public Health Association, Washington, DC, 1998.
[10] C.Y. Wu, P. Biswas, N.J. Fendinger, Model to assess heavy metal emission from municipal solid waste incineration, Hazard. Waste Hazard. Mater. 11 (1994) 71–92.
[11] M.Y. Wey, T.J. Fang, The effect of organic and inorganic chlorides on the formation of HC1 with various hydrogen containing sources in a fluidized bed incinerator, Environ. Int. 21 (1995) 423–431.
[12] K.S. Wang, K.Y. Chiang, S.M. Lin, C.C. Tsai, C.J. Sun, Effects of chlorides on emissions of hydrogen chloride formation in waste incineration, Chemosphere 38 (1999) 1571–1582.
[13] J. Abbasian, J.R. Wangerow, A.H. Hill, Effect of HCl on sulfidation of calcium oxide, Chem. Eng. Sci. 48 (1993) 2689–2695.